БЪЛГАРСКА АКАДЕМИЯ НА НАУКИТЕ • BULGARIAN ACADEMY OF SCIENCES

ГЕОХИМИЯ, МИНЕРАЛОГИЯ И ПЕТРОЛОГИЯ • 39 • СОФИЯ • 2002
GEOCHEMISTRY, MINERALOGY AND PETROLOGY • 39 • SOFIA • 2002

P-T metamorphic path of sillimanite-bearing schists in an extensional shear zone, Central Rhodopes, Bulgaria

Milena Georgieva, Zlatka Cherneva, Krastina Kolcheva, Stoian Sarov, Ianko Gerdjikov, Emilia Voinova

Abstract. Sillimanite-bearing schists are situated in an extensional shear zone in the NE periphery of the Central Rhodopian Dome, Bulgaria. Microstructural relationships distinguish several sequential mineral assemblages namely: garnet porphyroblast cores with inclusions of quartz, rutile, biotite and ilmenite; leucosome assemblage composed of plagioclase, K-feldspar and quartz; matrix assemblage composed of garnet porphyroblast rims, plagioclase, quartz, biotite, fibrolite, chlorite, muscovite and white hydromicas. Geothermometric and geobarometric results characterize changing metamorphic conditions: from kyanite stability field 620-640˚C / 7-8 kbar for garnet core assemblage formed in deeper crustal level (25–28 km), to sillimanite stability field 680-560˚C / 6-3 kbar for fibrolite-bearing matrix assemblage formed in shallower level (20–10 km) during continuous ductile and ductile-brittle deformation and fluid circulation.

Key words: fibrolite, thermobarometry, shear zone, Rhodopes
Addresses: M. Georgieva, Z. Cherneva, E. Voinova, S. Sarov – Geological Institute, Bulgarian Academy of Sciences, 1113 Sofia, Bulgaria; E-mail: milena@geology.bas.bg; K. Kolcheva, I. Gerdjikov – Sofia University, 1000 Sofia, Bulgaria

Георгиева, М., З. Чернева, К. Колчева, С. Саров, Я. Герджиков, Е. Войнова. 2002. Р-Т условия на метаморфизъм на силиманит-съдържащи шисти от екстензионната зона на срязване Канарата, Централнородопска подутина, България. - *Геохим., минерал. и петрол.,* **39**, 81-95.

Резюме. Силиманит-съдържащи шисти се разкриват в екстензионна зона на срязване в североизточната периферия на Централнородопската подутина в България. Микроструктурните взаимоотношения разграничават няколко последователни минерални асоциации: гранатови ядра с включения от кварц, рутил, биотит и илменит; асоциация в левкосомата, изградена от плагиоклаз, К-фелдшпат и кварц; асоциация в матрикса представена от периферията на едри гранатови порфиробласти, плагиоклаз, кварц, биотит, фибролит, хлорит, мусковит, бели хидрослюди. Термобарометричните резултати характеризират промяна в метаморфните условия от полето на стабилност на кианита 620-640˚C / 7-8 kbar за ядрата на гранатовите порфиробласти, образувани в по-дълбоко ниво на кората (25–28 km); към полето на стабилност на силиманита 680-560˚C / 6-3 kbar за фибролит-съдържащата асоциация на матрикса, образувана в по-плитко ниво (20–10 km) в условия на непрекъсната пластична и крехко-пластична деформация и флуидна циркулация.

Introduction

Sillimanite-bearing rocks are of great importance for understanding the metamorphic evolution. The presence of sillimanite usually testifies to high-temperature conditions and partial melting. On the other hand, fluid-assisted and deformation-induced reactions favour retrogressive formation of fibrolitic sillimanite in amphibolite facies shear zones (Vernon, 1979; Wintsch, Andrews, 1988; Digel et al., 1998; Musumeci, 2002). The findings of sillimanite-bearing schist in the Central Rhodopes are known long time ago. Kozhoukha-

rov et al. (1977) suggested the most probable values of *T* 620-660°C and *P* 4.3-7.2 kbar according to quartz-muscovite-sillimanite assemblage stability in sillimanite-bearing schists from the Ardino area. Although such kinds of rocks are good monitors of metamorphic histories no detailed studies have been performed later. We present our preliminary petrologic results on mineral chemistry and P-T estimates of sillimanite-bearing schists in the Kanarata extensional shear zone from the Northeastern parts of the Central Rhodope metamorphic complex. Representative samples of studied materials are deposited at the collections of the Geological Institute under № MER.1.2002.15.1-4.

Geological setting

Sillimanite-bearing schists crop out among migmatitic gneisses in close association with amphibolites and marbles in the Northeastern part of the Central Rhodopian Dome. The later have been described (Ivanov et al., 2000) as one of the largest Late Alpine swells, which formation was related to post-thickening extension and unroofing of high-grade metamorphic complexes in the Rhodopes. Recently Sarov and Gerdjikov (2002) have concluded that sillimanite-bearing schists mark a high-temperature extensional shear zone traced from NW to SE between the hamlets of Dve Topoli and Kanarata to the Dyavolski Most ("Devil's Bridge") at Arda River (Fig. 1). The zone

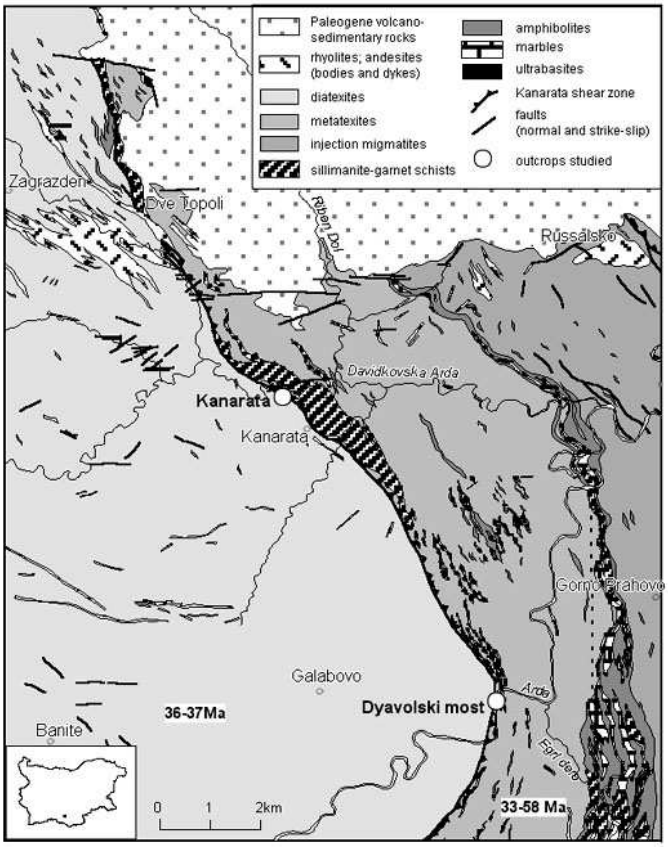

Fig. 1. Geologic map of the NE part of the Central Rhodopian Dome after Sarov and Gerdjikov (2002)
Фиг. 1. Геоложка карта на СИ част на Централнородопската подутина по Sarov & Gerdjikov (2002)

(named Kanarata) is 250-300 m wide and separates two different in style of migmatization parts of the section (diatexites in the footwall and metatexites in the hanging wall). Movements along the shear zone lead to unroofing of the diatexite core of the Central Rhodopian Dome. This interpretation is supported by similar U-Pb age determinations available for migmatites in both parts: 33-58 Ma (zircon, Arnaudov et al., 1990) in the hanging wall; 36.5-37 Ma (monazite, Peytcheva et al., 2000) and 37-38 Ma (monazite and zircon, Ovtcharova et al., 2002) in the footwall.

Our study considers two sillimanite-bearing schist localities situated in the valleys of Davidkovska and Arda rivers, and called in this paper respectively Kanarata and Dyavolski Most (Fig. 1). The schists include folded and dismembered aplite-pegmatite injection. The foliation and compositional migmatitic layering in the schists is parallel to the high-grade foliation in the surrounding migmatitic gneisses. Late movements along the foliation planes and small extensional faults have been followed by fluid circulation producing thin hematite or black manganese sheets (Sarov, Gerdjikov, 2002).

Petrography

Sillimanite-bearing schists consist of garnet, biotite, ± muscovite, quartz, plagioclase, ± K-feldspar, sillimanite, white hydromicas, chlorite, sagenite, and accessory graphite, rutile, ilmenite, apatite, zircon, monazite, tourmaline. K-feldspar, plagioclase, and quartz in variable proportions form millimeter- to centimeter-scale leucosome segregation. The later occurs as elongated lenses and boudinaged bands in a reddish-brown matrix of garnet, biotite, ± muscovite, plagioclase, and quartz. Garnet occurs as fractured and rotated zoned porphyroblasts (2-5 mm). Garnet cores include S_1 oriented exsolutions and inclusions of quartz, rutile, and biotite (Kanarata), or ilmenite (Dyavolski Most). Garnet fragments in the matrix are common. Small ($\leq$ 0.1 mm) euhedral garnet grains are included in the matrix plagioclase. Oriented biotite and minor muscovite, plagioclase, garnet, and quartz grains mark well-defined S_2 foliation. Biotite is the dominant mineral phase in the dark bands. It forms red coloured grains (1–3 mm size) deformed and partially replaced by late muscovite, chlorite + sagenite, sillimanite, and white hydromicas. Plagioclase is subhedral to anhedral and ranges from fine- to coarse-grained. Leucosome minerals are coarser-grained (to cm size), and elongated along the foliation, showing undulose extinction, and perthite, and anti-perthite exolutions in feldspars. Sillimanite occurs mostly as fibrolite mats fringing and embedding biotite or included in undeformed elongated quartz grains, as well as in strands and folia with c-axes preferred orientation along micro-shears in both matrix and leucosome. The progressive widening of the micro-shears led to zoned veinlets development composed of fibrolite inside and microcrystalline white hydromicas and chlorite along the periphery. Scarce fine grained prismatic sillimanite associates with coarse-grained undeformed quartz in separate elongated lenses. Migmatitic gneiss that crops out alternating the schists in the Kanarata shear zone also contains millimetre to centimetre scale fibrolite strands. The appearance of fibrolite is accompanied with red-coloured biotite similar to that in the sillimanite-bearing schists.

Microstructure relations mentioned above make it possible to distinguish several equilibrium mineral assemblages. An earlier one is composed of garnet porphyroblast cores with quartz, rutile, biotite, and ilmenite inclusions. The second one is composed of garnet porphyroblast rims, fine-grained euhedral garnet, and matrix biotite, plagioclase, quartz, ± muscovite, ilmenite, and graphite. The leucosome assemblage of quartz, plagioclase and K-feldspar formed contemporaneously. It lacks anhydrous peritectic phases and should be considered as a product of subsolidus mobilization or low temperature water-saturated melting in biotite stability field. Sillimanite crystallized after leucosome segregation. The bulk of fibrolite formed from biotite decomposition. The nucleation and growth of

Table 1. *Representative analyses of garnets: c – core; r – rim; f – fragment; i – inclusion in leucosome K-feldspar*
Таблица 1. *Представителни анализи на гранати: c – ядро; r- периферия; f – фрагмент; i – включение в К-фелдшпат от левкосома*

Location	Kanarata								Dyavolski Most							
Sample	7009-1I			7009-3I			7009-3L	7009-3M	M5		R17		M17A			
Point	1r	5c	9r	34r	39c	40r	6r	14f	27i	29i	20f	22f	7r	14r	12r	16c
SiO_2	36.93	37.69	37.46	37.74	37.54	36.83	36.08	35.99	36.87	37.12	35.35	35.91	36.47	37.22	36.58	36.51
TiO_2	-	-	0.04	-	-	0.03	-	0.12	-	0.11	0.06	-	-	0.31	0.17	0.10
Al_2O_3	20.90	21.20	20.91	21.12	20.75	20.25	21.52	20.89	20.78	20.78	20.84	20.65	20.78	21.32	21.51	20.84
FeO	24.64	28.90	25.42	23.57	25.77	24.08	22.97	23.61	25.27	24.10	28.28	29.54	27.57	27.89	28.76	30.32
Cr_2O_3	0.23	0.02	0.06	0.03	-	-	0.05	-	0.26	0.01	-	-	-	-	0.19	0.10
MnO	14.49	6.37	12.97	14.55	12.08	14.27	14.26	13.21	12.06	14.38	10.14	8.17	12.41	11.02	9.67	8.22
MgO	2.17	4.07	2.91	2.31	2.95	2.34	2.83	3.23	2.92	2.43	2.23	2.29	1.21	1.7	2.37	1.72
CaO	1.15	1.74	1.06	1.28	1.19	1.28	1.46	1.41	1.28	1.16	1.29	1.34	1.41	1.27	0.83	1.20
Na_2O	-	-	-	-	-	-	0.31	0.41	-	-	0.30	0.11	-	-	-	-
Σ	100.51	99.99	100.83	100.60	100.28	99.08	99.48	98.98	99.44	100.09	98.52	98.05	99.99	100.91	100.08	99.01
Alm	44.93	64.45	55.57	53.49	56.65	52.67	43.05	42.67	46.89	53.62	54.19	58.41	52.29	63.81	57.55	70.11
Grs	3.15	4.91	2.87	3.62	3.48	3.83	4.80	4.52	3.54	3.35	4.64	4.91	4.89	3.14	2.24	3.23
Prp	10.64	16.18	11.71	9.34	11.98	9.74	13.45	15.76	14.50	9.85	11.46	12.06	6.54	6.93	11.89	7.09
Sps	40.37	14.39	29.65	33.44	27.88	33.76	38.51	36.62	34.03	33.14	29.59	24.45	36.00	25.54	27.56	19.25
Fe/(Fe+Mg)	0.86	0.80	0.83	0.85	0.83	0.85	0.82	0.80	0.83	0.85	0.88	0.88	0.92	0.90	0.87	0.91

Table 2. *Representative analyses of biotites: m - matrix; i – inclusion*
Таблица 2. *Представителни анализи на биотити: m – матрикс; i – включение*

Location	Kanarata											Dyavolski Most				
Sample	7009-1I			7009-3I			7009-3L	7009-3M	M3C	M5	M30	M17A			R17	
Point	10m	13i	17m	35m	37i	38m	9	15m	21m	32i	33m	5m	6m	13m	19m	26m
SiO_2	36.24	36.74	35.88	35.44	36.21	36.49	35.60	35.50	36.02	36.20	35.78	33.82	33.82	33.96	34.50	34.35
TiO_2	2.82	2.08	2.68	2.51	3.48	2.3	2.68	2.29	3.53	3.19	2.88	3.94	3.94	3.16	2.28	2.72
Al_2O_3	20.26	21.23	20.16	19.89	19.64	20.74	20.77	20.52	16.07	19.69	17.71	20.22	20.22	20.60	20.81	20.92
Cr_2O_3	0.35	0.13	0.24	0.11	0.38	-	0.09	0.16	0.17	0.06	0.13	0.04	0.04	-	0.06	0.13
FeO	16.52	14.85	16.74	17.18	16.01	17.46	16.10	16.33	20.64	16.95	19.75	21.12	21.12	22.69	20.70	20.31
MnO	0.40	0.11	1.00	0.71	0.34	0.79	0.6	0.69	0.68	0.79	0.69	0.79	0.79	0.79	0.41	0.31
MgO	8.83	10.78	8.99	9.49	9.71	10.14	10.38	9.74	9.96	8.87	10.10	6.02	6.02	6.29	7.56	7.70
BaO	-	0.19	0.07	0.05	0.14	-	-	0.24	-	-	-	-	-	-	0.04	-
CaO	0.02	0.09	0.11	0.04	-	0.04	-	0.22	-	0.04	-	0.35	0.35	0.17	-	-
Na_2O	0.18	0.58	0.45	0.18	0.10	0.35	0.72	0.50	0.18	0.32	0.11	0.56	0.56	0.30	0.52	0.69
K_2O	9.48	9.26	9.53	9.24	9.34	9.06	9.51	9.26	9.45	9.55	9.55	8.89	8.89	8.89	9.12	8.63
Σ	95.06	96.04	95.85	94.84	95.15	97.37	96.45	95.45	96.70	95.66	96.70	95.75	95.05	96.85	96.00	95.76
^{IV}Al	2.56	2.59	2.62	2.63	2.58	2.64	2.72	2.66	2.53	2.57	2.60	2.81	2.81	2.82	2.75	2.78
^{VI}Al	1.03	1.09	0.95	0.92	0.88	0.95	0.91	0.97	0.35	0.92	0.55	0.85	0.85	0.88	0.98	0.96
Fe/(Fe+Mg)	0.51	0.44	0.51	0.50	0.48	0.49	0.47	0.48	0.54	0.52	0.52	0.66	0.66	0.67	0.61	0.60

fibrolite together with matrix retrogression minerals such as white hydromicas and chlorite, and undeformed quartz completes a late-stage assemblage closely related to brittle-ductile micro-shear zones.

Mineral chemistry

Mineral chemistry varies systematically in both localities showing higher Fe concentrations in the mafics from the Dyavolski Most outcrops. All the garnets have spessartine-almandine composition (Table 1). Zoned garnets (Fig. 2a) display decrease in Mg and Fe, and increase in Mn content from core to rim. The outer rims show typical retrograde drop in Mg. Low-temperature reequilibration of the rims is marked by higher Fe/(Fe+Mg) value compared to the core. Small euhedral garnet grains correspond to the porphyroblasts' rims (Fig. 2b). Garnet core fragments do not show full reequilibration when armoured by matrix biotite. This testifies to fast operating and incomplete matrix reactions.

Biotite is enriched in siderophyllite (Dyavolski Most) or eastonite (Kanarata) component (Table 2, Fig. 3). The Fe/(Fe+Mg) ratio shows large variation keeping lower values in biotite inclusions within garnet cores and within leucosome feldspars as compared to matrix biotite. High Al content in both structural positions distinguishes red coloured biotite of sillimanite-bearing rocks from brown coloured one of common migmatites in the area. The later is represented by biotite from the hanging wall Egri Dere migmatites (Cherneva et al., 1997). There is a systematic inverse relationship between Ti concentration and Mg/(Mg+Fe). The maximal Ti contents in biotite, both in the schists and migmatites, are 0.35–0.45 *apfu* for XMg values 0.30–0.45, corresponding to high temperature metamorphic conditions above the second sillimanite isograd (Henry, Guidotti, 2002).

K-feldspar $Or_{75–85}$ and plagioclase $An_{17–26}$ are common in leucosome segregations. Matrix plagioclase (Table 3) has similar compositional variation $An_{15–30}$ dominated by An_{20-26}.

Ilmenite is Mn-rich. Matrix ilmenite has relatively lower Mn content compared to ilmenite inclusions within garnet core (respectively 3.4–4 and 6.1–7.7 wt % MnO; Table 4).

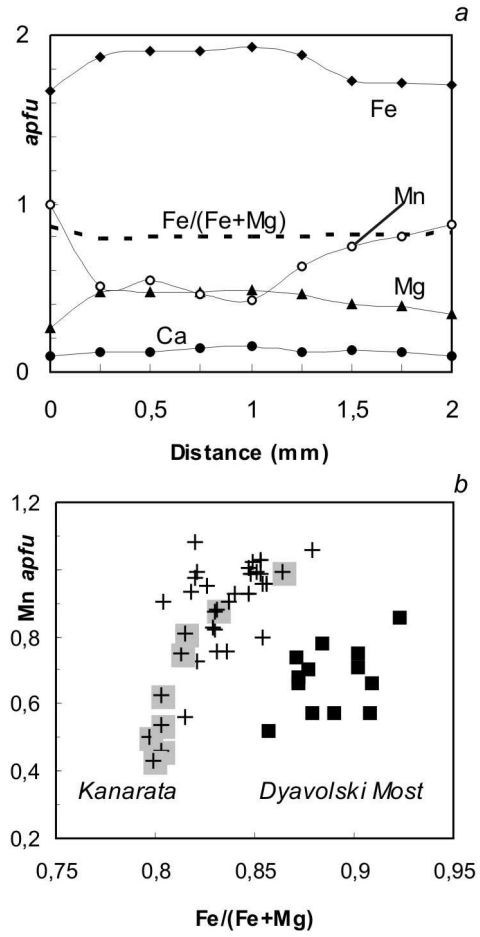

Fig. 2. Garnet composition: *a* – zoned porphyroblast (sample 7009-1I; Kanarata outcrop); *b* - main trend of Mg, Fe and Mn distribution; marked crosses show zoned porphyroblast compositional variation

Фиг. 2. Състав на граната: *а* – зонален порфиробласт (обр. 7009-1I; Канарата); *б* – главен тренд в разпределението на Mg, Fe и Mn; маркираните кръстчета показват вариацията в състава на зоналния порфиробласт

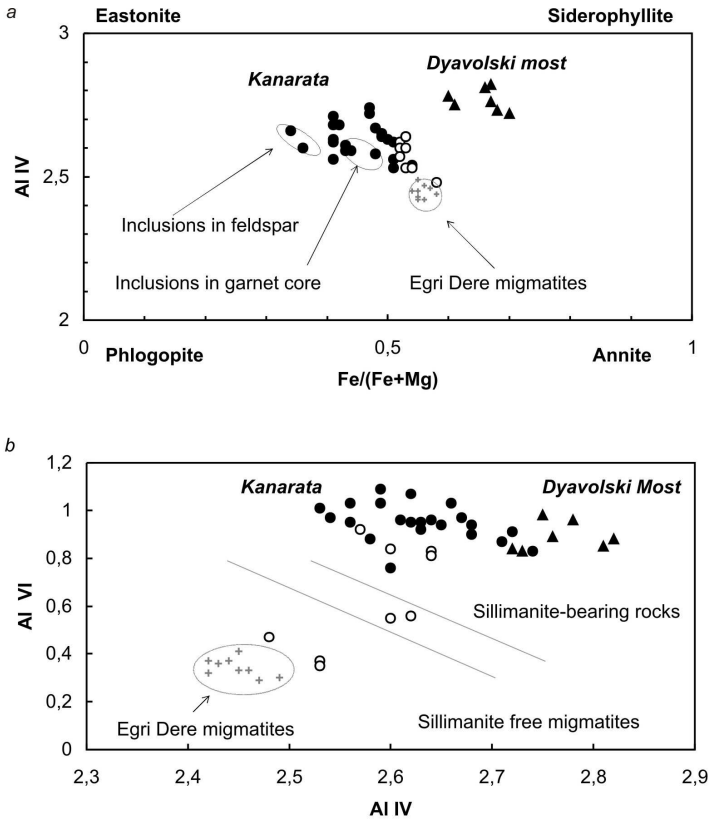

Fig. 3. Biotite composition: *a* – classification diagramm; *b* – a comparison between sillimanite schists and migmatites from the shear zone, and migmatites from the hanging wall (Egri Dere)
Фиг. 3. Състав на биотита: *а* – класификационна диаграма; *б* – съпоставка на силиманитови шисти и мигматити от зоната на срязване с мигматити от висящото крило (Егри дере)

Mn-rich phases as garnet, ilmenite and even biotite (up to 1% MnO) focus attention on the chemical system that is Mn-rich too. Mn stabilizes garnet to substantially lower temperatures and pressures (Spear, 1993) and depletes the amount of Al available to staurolite, thus restricting staurolite stability field (Tinkham et al., 2001).

Thermobarometry

Thermobarometric calculations have been performed using different calibrations of garnet-biotite geothermometers (including equations for Mn-correction), garnet-plagioclase-sillimanite-quartz (GASP), and garnet-rutile-ilmenite-Al_2SiO_5-quartz (GRAIL) geobarometers. Selected garnet and biotite compositions used for thermobarometric estimates are shown in Tables 1 and 2. Matrix plagioclase An_{20-26} (Table 3) and ilmenite inclusions in zoned garnet (Table 4) have been used in GASP (Hodges, Crowley, 1985) and GRAIL (Bohlen et al., 1983) geobarometry respectively. The uncertainties associated with thermometry correction for Mn content in garnet (Ganguly, Saxena, 1984; Perchuk, 1981) are substantial for matrix garnet-biotite pairs containing Mn-rich garnet and Ti-rich biotite. The results obtained from these calculations show

considerable differences of over 100°C, being in the range 700-750°C and 580-650°C respectively. The temperatures calculated from

Table 3. *Representative analyses of plagioclases*
Таблица 3. *Представителни анализи на плагиоклаз*

Location	Kanarata					Dyavolski Most		
Sample	7009-1I		7009-3L	7009-3M	M5	M17A	R17	
Point	12	18	7	16	31	3	18	24
SiO_2	60.68	62.46	61.21	62.17	61.58	60.57	60.14	61.40
TiO_2	-	-	-	-	-	-	0.15	0.06
Al_2O_3	23.69	23.23	24.75	24.21	23.60	25.15	25.77	24.08
FeO	0.37	0.17	0.13	0.47	-	0.16	0.30	0.26
MgO	-	-	-	-	-	-	-	-
BaO	0.02	-	-	0.02	-	0.12	-	-
CaO	5.22	4.40	5.46	4.69	4.89	6.23	6.21	5.18
Na_2O	9.11	9.63	8.01	7.98	9.38	7.89	7.52	8.18
K_2O	0.35	0.12	0.43	0.42	0.19	0.10	0.15	0.34
Σ	99.44	100.00	99.99	99.96	99.64	100.20	100.50	99.50
Ab	74.50	79.30	70.80	73.50	76.80	69.10	68.10	72.60
An	23.60	20.00	26.70	23.90	22.20	30.10	31.10	25.50
Or	1.90	0.70	2.50	2.60	1.00	0.60	0.80	2.00
Cn	-	-	-	-	-	0.20	-	-

the thermometers of Ferry and Spear (1978, modified by Hodges and Spear, 1982) are in accord with the petrographic arguments. Ignoring the extreme cases mentioned above, we base further interpretation on coinciding results obtained from all cited geothermometers and show on Fig. 4 those from the equation of Hodges and Spear (1982).

Assuming similar conditions during garnet core assemblage formation in both localities, we join together temperature estimates of Kanarata and pressure estimates of Dyavolski Most samples. Matrix assemblage estimates include zoned garnet rims and matrix biotite and plagioclase. The results characterize changing metamorphic conditions: from kyanite stability field 620-640˚C / 7–8 kbar for garnet porphyroblast cores with biotite and ilmenite inclusions; to sillimanite stability field 680-560˚C / 6-3 kbar for matrix minerals and garnet porphyroblast rims (Fig. 4).

Table 4. *Ilmenites from the matrix assemblage (m) and inclusions in garnet cores (i); sample M17A*
Таблица 4. *Илмениm от асоциацията на матрикса (m) и включения в гранатовите ядра (i); обр. M17A*

Point	8m	10m	11i	17i
TiO_2	50.01	52.60	52.64	50.38
Cr_2O_3	0.10	0.23	0.03	0.14
FeO	43.81	43.07	39.60	42.20
MnO	3.97	4.02	7.37	6.15
MgO	0.31	0.08	-	0.22
Σ	98.2	100.00	100.00	99.10

Discussion

P-T estimates trace a decompression path corresponding to the extensional signatures of the shear zone and crossing several metamorphic reactions lines on the petrogenetic grid (Fig. 4). The first group of results marks metamorphic conditions both in kyanite and staurolite stability fields just above the water-saturated solidus

$Ms + Kfs + Qtz + Ab + H_2O = melt$ (1).

According to our observations kyanite occurs in metapelites out of the shear zone. The major elements Fe, Mg and Mn diffuse sufficiently rapidly at the *P-T* conditions of partial melting (Spear et al., 1999), therefore diffusion reequilibration of biotite inclusions in garnet

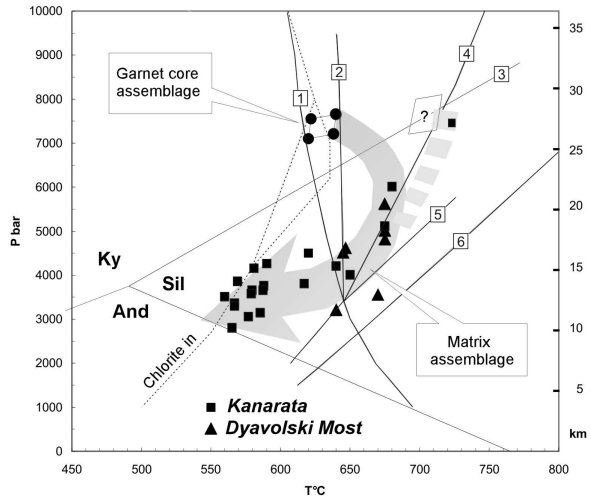

Fig. 4. *P-T* metamorphic conditions calculated for sillimanite-bearing schists from the Kanarata extensional shear zone: reactions 1, 2, 4, 5, and 6 after Thompson (2001); dashed lines mark staurolite and chlorite fields in the system MnNCKFMASH after Tinkham et al. (2001); kyanite, sillimanite, and andalusite stability fields after Holdaway (1971)

Фиг. 4. *P-T* условия на метаморфизъм определени в силиманитсъдържащи шисти от екстензионната зона Канарата: реакции 1, 2, 4, 5 и 6 по Thompson (2001); пунктир маркира полето на ставролита и хлорита в системата MnNCKFMASH по Tinkham et al. (2001); полета на стабилност на кианит,силиманит и андалузит по Holdaway (1971)

cores should be assumed. We have modified the composition of one garnet-biotite pair (Grt5c – Bt13i; sample 7009-1I; Table 1 and 2) assuming Mg and Fe exchange of 0.05 *apfu* and changing Fe/(Fe+Mg) ratio of both minerals from 0.8 and 0.44 to 0.78 and 0.45, respectively. Calculated temperatures form a hypothetical (question-marked on Fig. 4) field above the reaction

$Ms + Ab + Qtz + H2O = Al_2SiO_5 + melt$, (2)

close to the conversion

$Ky = Sil$ (3)

and close to muscovite dehydration melting reaction

$Ms + Ab + Qtz = Kfs + Sil + melt$ (4).

Similar results 723°C / 7.4 kbar (Fig. 4) have been obtained for garnet core fragments preserved in matrix biotite bands (Grt14 – Bt15, sample 7009-3M). Dehydration melting is supported by matrix temperatures coinciding with reaction line (4) at 680-660˚C / 6-4.5 kbar (Fig. 4), that testifies to possible formation of peraluminous melts during migmatization. The presence of graphite reducing aH_2O (Spear, 1993) should support dehydration reaction. Dehydration melting in presence of graphite leaves the graphite content of the rock virtually unchanged (Cesare, 1995). The above reactions (1, 2, and 4) suggest muscovite consumption that accounts for low abundance of primary muscovite in the schists. The path trajectory (grey arrow, Fig. 4) traced between measured core assemblage field and matrix thermal peak indicates a temperature increase of 40°C, and should be considered as an indication of frictional heating in the shear zone. The garnet zoning profile (flat Fe/(Fe+Mg) line, Fig. 2 a) however, do not support such an interpretation. It is more consistent with isothermal decompression followed by cooling during matrix retrogression.

Matrix retrogression occurs below the water-saturated solidus (650°C / 4.5–3 kbar) trending to lower temperatures (560˚C / 3.8–

2.8 kbar) in chlorite stability field. Sillimanite crystallized after leucosome segregation when considerable fluid release by crystallizing melt was possible. As shown by Musumeci (2002) sillimanite growth is strongly favoured by fluid action at the grain scale along pre-existing planes of weakness. Such processes are well understood in retrograde shear zones under greenschist and amphibolite facies conditions (Bell, Cuff, 1989; McCaig, 1987). We should assume an operation of back reaction between melt and restitic phases

$Ms + Qtz + melt = Kfs + Sil + H_2O$ (5)

at 670-640˚C / 3.5-3.2 kbar (Fig. 4) as some pressure values are low enough. Microstructure features however, show sillimanite growth replacing biotite, and quartz and white hydromicas as product phases in association with sillimanite. Several authors have proposed metasomatic reactions due to base-cation leaching of biotite by hydrogen metasomatism (Vernon, 1979)

$2K(Mg,Fe)_3AlSi_3O_{10}(OH)_2 + 14H^+ = Al_2SiO_5 + 5SiO_2 + 2K^+ + 6(Mg,Fe)_2 + 9H_2O$,

or acidic fluid circulation (Kerrick, 1987; Digel et al., 1998)

$2K(Mg,Fe)_3AlSi_3O_{10}(OH)_2 + 14HCl = Al_2SiO_5 + 5SiO_2 + 2KCl + 6(Mg,Fe)Cl_2 + 9H_2O$

in a system open to non-volatile components (Wintsch, Andrews, 1988). The authors cited emphasise the absence or low abundance of quartz and K-bearing minerals as product phases assuming metasomatic transfer and loss of cations. In our examples the occurrence of Fe and Mn hydroxides along the foliation planes and small extensional faults corroborates cation leaching during fluid circulation. The components have not been completely removed. The white hydromicas and quartz may have provided a local sink for K and Si released from biotite decomposition.

The association of sillimanite-bearing rocks with migmatites may be significant in as much as associated aqueous solutions of magmatic origin may have been involved in the reactions (Vernon, 1979). Sillimanite growth late in the metamorphic history and restricted close to the shear zone brings to mind the positive relationships between mineral occurrence, extensional deformation and fluid release along the shear zone.

It is worth noting that some results for the matrix approximate cordierite stability field marked by the reaction

$Bt + Ab + Sil + Qtz = Crd + Grt + Kfs + melt$ (6).

Nevertheless cordierite has been not found in sillimanite-bearing schists, cordierite-and andalusite-bearing pegmatites that cut the metamorphic rocks are well known (Kostov, 1954) in the locality Dyavolski Most. Their formation is thought to be due to the action of fluids which have caused a mobilization of constituents from the crystalline series.

The estimates of *P-T* conditions characterize the Kanarata extensional shear zone metamorphic path. The formation of the zone followed the thermal peak of migmatization in both footwall and hanging wall of the section. Decompression path described above corresponds to depth change of more than 10 km (Fig. 4). Garnet core assemblage formed in deeper crustal level between 25 and 28 km. Matrix assemblage formed in shallower level between 20 and 15 km at high-temperature conditions above the water-saturated solidus. Matrix retrogression occurred at a depth of 15–10 km and decreasing temperature from 650 to 560ºC. Fluid-assisted deformation within the extensional shear zone produced sillimanite as a component of the matrix retrogression assemblage in amphibolite facies conditions

The results do not allow to calculate reliable thermal peak of melting during migmatization, nevertheless several possible melting reactions including dehydration melting one have been proposed. Additional investigations on the schists outside the shear zone should help to clarify the conditions of garnet core assemblage formation, which strongly affect the *P-T* path trajectory.

Sillimanite appearance in the shear zone rocks both schist and alternating migmatitic gneiss supports an interpretation of open system process that seems consistent with the assumption of Sarov and Gerdjikov (2002) for schists “derived at the expense of host migmatized metagranitoids”. However, numerous observations support sedimentary protolith

origin namely: the schists outside the shear zone have similar mineral assemblages; graphite is a common compound; sillimanite-bearing schists closely associate with marbles.

Conclusions

The metamorphic *P-T* path of the Kanarata shear zone is consistent with extensional decompression at high temperature amphibolite facies conditions and a depth change of about 10 km. Sillimanite-bearing schists mineral assemblages display changing metamorphic conditions: from kyanite stability field 620-640˚C / 7-8 kbar for garnet core assemblage formed in deeper crustal level to sillimanite stability field 680-560˚C / 6-3 kbar for fibrolite-bearing matrix assemblage formed in shallower level during continuous ductile and brittle-ductile deformation and fluid circulation.

References

Arnaudov, V., B. Amov, Z. Cherneva, R. Arnaudova, M. Pavlova, E. Bartnitsky. 1990. Petrological-geochemical and lead-isotope evidence of Alpine metamorphism in the Rhodope crystalline complex. - *Geol. Balcanica*, **20**, 5, 29-44.

Bell, T.H., C. Cuff. 1989. Dissolution, solution transfer, diffusion versus fluid flow and volume loss during deformation/metamorphism. – *J. Metam. Geol.*, **7**, 425-447.

Bohlen, S.R., V.J. Wall, A.L. Boettcher. 1983. Experimental investigation and geological applications of equilibria in the system FeO-TiO_2-Al_2O_3-SiO_2-H_2O. - *Amer. Mineral.*, **68**, 1049-1058.

Cesare, B. 1995. Graphite precipitation in C-O-H fluid inclusions: Closed system compositional and dencity changes, and thermobarometric implications. - *Contrib. Mineral. Petrol.,* **122**, 25-33.

Cherneva, Z., R. Arnaudova, Tz. Iliev, K. Rekalov. 1997. Feldspar thermometry of migmatitic formations from the Central Rhodopes. – *Rev. Bulg. Geol. Soc.,* **58**, 3, 139-156 (in Bulgarian).

Digel, S.G., E.D. Ghent, P.S. Simony. 1998. Early Cretaceous kyanite-sillimanite metamorphism and Paleocene sillimanite overprint near Mount Cheadle, southeastern British Columbia: Geometry, geochronology, and metamorphic implications. - *Can. J. Earth Sci.,* **35**, 1070-1087.

Ferry, J.M., F.S. Spear. 1978. Experimental calibration of the partitioning of Fe and Mg between biotite and garnet. – *Contrib. Mineral. Petrol.,* **66**, 113-117.

Ganguly, J., S.K. Saxena. 1984. Mixing properties of alumosilicate garnets: Constraints from natural and experimental data, and applications to geothermobarometry. - *Amer. Mineral.*, **69**, 88-97.

Henry, D.J., C.V. Guidotti. 2002. Titanium in biotite from metapelitic rocks: Temperature effects, crystal-chemical controls, and petrologic applications. – *Amer. Mineral.*, **87**, 375-382.

Hodges, K.V., F.S. Spear. 1982. Geothermometry, geobarometry and the Al_2SiO_5 triple point at Mt. Moosilauke, New Hampshire. - *Amer. Mineral.*, **67**, 1118-1134.

Hodges, K.V., P.D. Crowley. 1985. Error estimation and empirical geothermobarometry for pelitic systems. - *Amer. Mineral.*, **70**, 702-709.

Holdaway, M.J. 1971. Stability of andalusite and aluminium silicate phase diagram. - *Am. J. Sci*., **271**, 20-47.

Ivanov, Z. 2000. Tectonic position, structure and tectonic evolution of Rhodope massif – In: *Gide to Excursion B*. ABCD–GEODE Workshop*,* Borovets, Bulgaria, 1-5.

Kostov, I. 1954. Andalusite in pegmatite from Ardino, Central Rhodopian Mountains. – *Ann. Univ. Sofia, Fac. Biol.-Geol.-Geogr., 2 - Geol.,* **48**, 1-22 (in Bulgarian).

Kozhoukharov, D., E. Kozhoukharova, L. Grozdanov. 1977. Temperature and pressure during the metamorphism of the Precambrian complexes from the Rhodope massif. – *Geol. Balcanica,* **7**, 3, 103-116.

McCaig, A.M. 1987. Deformation and fluid-rock interaction in metasomatic dilatand shear bands. – *Tectonophysics*, **135**, 121-132.

Musumeci, G. 2002. Sillimanite-bearing shear zones in syntectonic leucogranite: Fluid-assisted brittle-ductile deformation under amphibolite facies conditions. – *J. Struct. Geol.*, **24**, 1491-1505.

Ovtcharova, M., Z. Cherneva, A. von Quadt, I. Peytcheva. 2002. Migmatitic geochronology and geochemistry: A key to understanding the exhumation of the Madan dome (Bulgaria). – *Goldschmidt Conference Abstracts 2002,* A537.

Perchuk, L.L. 1981. Correction of biotite-garnet thermometer for the case of Mn = Mg + Fe

isomorphism in garnet. - *Dokl. Acad. Nauk SSSR,* **256**, 2, 441-442 (in Russian).

Peytcheva, I., E. Salnikova, Y. Kostitsin, M. Ovtcharova, S. Sarov. 2000. Metagranites from the Madan-Davidkovo dome, Central Rhodopes: U-Pb and Rb-Sr protholite and metamorphism dating. - In: *Geodynamics and Ore Deposits Evolution of the Alpine-Balkan-Carpathian-Dinaride Province.* ABCD-GEODE Workshop, Borovets, Bulgaria, Abstracts, p. 66.

Sarov, S., I. Gerdjikov. 2002. Unroofing the Central Rhodopian dome from the East-Kanarata extensional shear zone. - *C. R. Acad. bulg. Sci.*, **55**, 2, 71-74.

Spear, F.S. 1993. *Metamorphic Phase Equilibria and Pressure-Temperature-Time Paths.* Washington, Min. Soc. Am., 799 p.

Spear, F.S., M.J. Kohn, J.T. Cheney. 1999. P-T paths from anatectic pelites. – *Contrib. Mineral. Petrol.*, **134**, 17-32.

Thompson, A. B. 2001. Clockwise P-T paths for crustal melting and H_2O recycling in granite source regions and migmatite terrains. – *Lithos*, **56**, 33-45.

Tinkham, D.K., C.A. Zuluaga, H.H. Stowell. 2001. Metapelite phase equilibria modeling in MnNCKFMASH: The effect of variable Al_2O_3 and MgO/(MgO+FeO) on mineral stability. – *Geol. Materials Res.*, **3**, 1, 1-42.

Vernon, R.H. 1979. Formation of late sillimanite by hydrogen metasomatism (base-leaching) in some high-grade gneisses. – *Lithos*, **12**, 143-152.

Wintsch, R.P., M.S. Andrews. 1988. Deformation induced growth of sillimanite: "stress" minerals revisted. – *J. Geol.*, **96**, 143-161.

Accepted December 28, 2002
Приета на 28.12.2002 г.